

CONF-80111--17

LASER ANNEALING OF ION IMPLANTED SILICON*

C. W. White, B. R. Appleton
Solid State Division, Oak Ridge National Laboratory
Oak Ridge, Tennessee 37830

and

S. R. Wilson
Motorola, Inc., Phoenix, Arizona 85008

MASTERSummary

Pulsed laser annealing of ion implanted silicon leads to the formation of supersaturated alloys by nonequilibrium crystal growth processes at the interface occurring during liquid phase epitaxial regrowth. The interfacial distribution coefficients from the melt (k') and the maximum substitutional solubilities (C_S^{\max}) are far greater than equilibrium values. Both k' and C_S^{\max} are functions of growth velocity. Mechanisms limiting substitutional solubilities are discussed.

Introduction

Extensive investigations have shown that radiation from high power lasers can be used to advantage in processing ion implanted semiconductors.¹⁻³ By using radiation from pulsed lasers it is possible to completely anneal extended defects in ion implanted semiconductors,⁴ to transform amorphous to single crystal layers,⁵ to dissolve precipitates in the near surface region,⁶ and to promote in diffusion of dopants deposited on the surface of semiconductors.⁷ Interest in laser annealing came about because of the very desirable advantages it offers over conventional thermal annealing and because laser annealing can be used to prepare materials with properties which cannot be achieved by conventional methods.⁸

In this paper we discuss the formation of supersaturated, substitutional alloys in silicon as a result of the rapid liquid phase epitaxial regrowth caused by pulsed laser annealing.⁹⁻¹¹ During pulsed laser annealing, it is believed that the absorbed laser light leads to melting of the near surface region¹² (to a depth of several thousand angstroms) followed by liquid phase epitaxial regrowth from the underlying substrate at velocities that are predicted to be several meters/sec.¹³ At these velocities,

*Research sponsored by the Division of Materials Sciences, U. S. Department of Energy under contract W-7405-eng-26 with Union Carbide Corporation.

DISCLAIMER

This book was prepared as an account of work sponsored by an agency of the United States Government. Neither the United States Government nor any agency thereof, nor any of their employees, makes any warranty, express or implied, or assumes any legal liability or responsibility for the accuracy, completeness, or usefulness of any information, apparatus, product, or process disclosed, or represents that it would necessarily be received by the intended recipient, or that it would be used for any specific purpose without infringing on any existing patent rights. Reference herein to any specific commercial product, process, or service by trade name, trademark, manufacturer, or otherwise, does not necessarily constitute or imply its endorsement, recommendation, or approval by the United States Government or any agency thereof. The views and opinions of authors expressed herein do not necessarily state or reflect those of the United States Government or any agency thereof.

recrystallization of the melted region takes place under conditions that are far from equilibrium at the interface.⁹ Group (III,V) dopants are incorporated into substitutional lattice sites at concentrations that can far exceed equilibrium solubility limits. Values for the interfacial distribution coefficient (k') during regrowth (defined as $k' = C_S/C_L$ where C_S and C_L are dopant concentrations in the solid and liquid phase at the interface) can be determined by comparing model calculations to experimental measurements of dopant concentration profiles after annealing. Values for k' are significantly larger than corresponding equilibrium values (k_0).⁹ For each dopant, there is a maximum concentration (C_S^{\max}) which can be incorporated into substitutional lattice sites as a result of pulsed laser annealing and values for C_S^{\max} far exceed equilibrium solubility limits (C_S^0).⁹ Both k' and C_S^{\max} are found to be functions of growth velocity. Finally we discuss the mechanisms limiting substitutional solubility and we compare measurements of C_S^{\max} obtained at two different growth velocities with recent predictions of thermodynamic limits for solute solubility in silicon at infinite growth velocity.¹⁴

Experimental Details

Group (III,V) dopants (B,Ga,In,As,Sb,Bi) were implanted into (100) Si single crystals at energies in the range 35 keV to 250 keV, and at doses in the range 10^5 to $10^{17}/\text{cm}^2$. Implanted crystals were annealed using the Q-switched output of a pulsed ruby laser (15×10^{-9} sec pulse duration time) at energy densities in the range 1-2 J/cm². Crystals were examined before and after laser annealing using 2.5 MeV He⁺ Rutherford backscattering and ion channeling measurements to determine the dopant concentration profile before and after laser annealing and the substitutional dopant concentration as a function of depth after annealing. Dopant profiles after laser annealing were compared to calculations using a model which incorporates liquid phase diffusion during epitaxial regrowth and a distribution coefficient from the melt (k'). Details of these calculations are given in Ref. 9. From this comparison values for k' during regrowth were determined. For crystals implanted to high doses, backscattering and channeling measurements were used to compare the total dopant concentration profile and the substitutional dopant profile as a function of depth after annealing. From this comparison, values for the limiting substitutional solubility C_S^{\max} were determined.

Experimental Results

Formation of Supersaturated Alloys By Laser Annealing

Figure 1 shows results for the case of Bi in Si after laser annealing. Laser annealing causes ~15% of the Bi to be segregated or zone refined to the

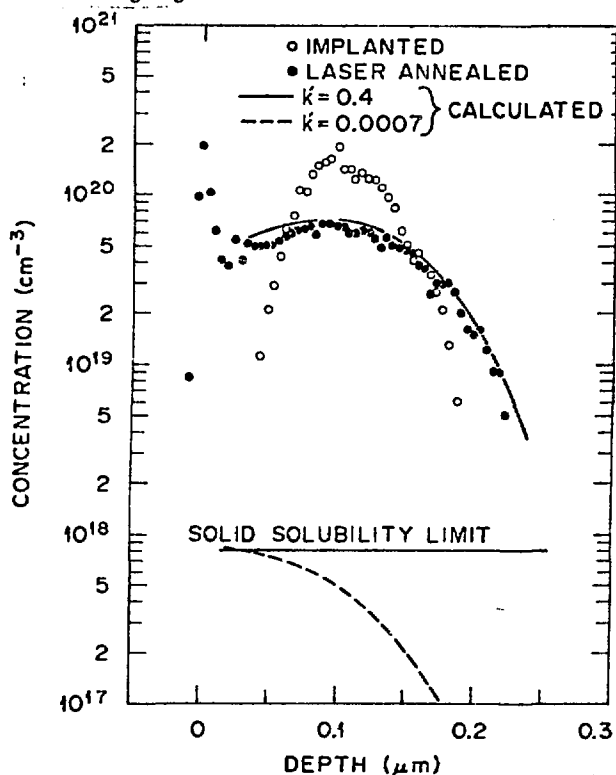


Figure 1. Profiles for ^{109}Bi (250 keV, $1.2 \times 10^{15}/\text{cm}^2$) in (100) Si Compared to Calculations.

Table I. Comparison of Laser Annealing Induced Distribution Coefficients (k') and Maximum Substitutional Solubilities (C_S^{max}) to Equilibrium Values (k_0 and C_S^0) of Ref. 16.

Dopant	k_0	k'	C_S^0 (cm^{-3})	C_S^{max} (cm^{-3})
As	0.3	1.0	1.5×10^{21}	5.0×10^{21}
Sb	0.023	0.7	7×10^{19}	1.3×10^{21}
Bi	0.0007	0.4	8×10^{17}	4×10^{20}
Ga	0.008	0.2	4.5×10^{19}	4.5×10^{20}
In	0.0004	0.15	8×10^{17}	1.5×10^{20}

surface, but ion channeling measurements show that the Bi remaining in the bulk of the crystal is >95% substitutional even though the maximum Bi concentration in the bulk exceeds the equilibrium solubility limit by a factor of ~100. This demonstrates the formation of a supersaturated solid solution during laser annealing. The solid line is a calculated profile using a value for k' of 0.4 and the fit to the data is reasonable. By contrast, the equilibrium value¹⁶ for the distribution coefficient (k_0) is 8×10^{-4} and if regrowth occurred under conditions of local equilibrium at the interface, the dotted line would be the expected profile in the bulk and almost all of the Bi would be segregated to the surface. Clearly, this does not fit the experimental data.

Table I summarizes our determined values for k' and compares them with equilibrium values (k_0).⁹ In each case k' is significantly greater than k_0 , reflecting the nonequilibrium nature of the laser annealing induced liquid phase epitaxial regrowth process. Deviation from equilibrium at the interface are brought about by the high regrowth velocity (~4.5 m/sec). These are the first measurements of distribution coefficients under conditions of nonequilibrium crystal growth for any system.

Values for the distribution coefficient during regrowth should be a strong function of growth velocity. Figure 2 shows that this is the case. These results were obtained by laser annealing Si crystals implanted by ²⁰⁹Bi while maintaining the substrate at three different temperatures during annealing in order to vary the growth velocity. Annealing with the substrate at 600°K leads to reduced thermal gradients and a lower growth velocity (~1.5 m/sec). At temperatures of 100°K the thermal gradients are steeper and the growth velocity is larger (~6.0 m/sec). Figure 2 shows that at high substrate temperatures (low growth velocity) a large fraction of the implanted Bi (~55%) is segregated to the surface during laser annealing. The distribution coefficient under these conditions is ~0.1. At low substrate temperatures (high growth velocity), only ~5% of the Bi is segregated to the surface and the distribution coefficient is ~0.5. These results demonstrate that as the growth velocity is decreased, more of the Bi is segregated to the surface, with a corresponding reduction in the value for k' .

Maximum Substitutional Solubilities

For each dopant, there is a maximum concentration which can be incorporated substitutionally into the lattice during laser annealing.⁹ This is illustrated in Fig. 3 for the case of In implanted into silicon,

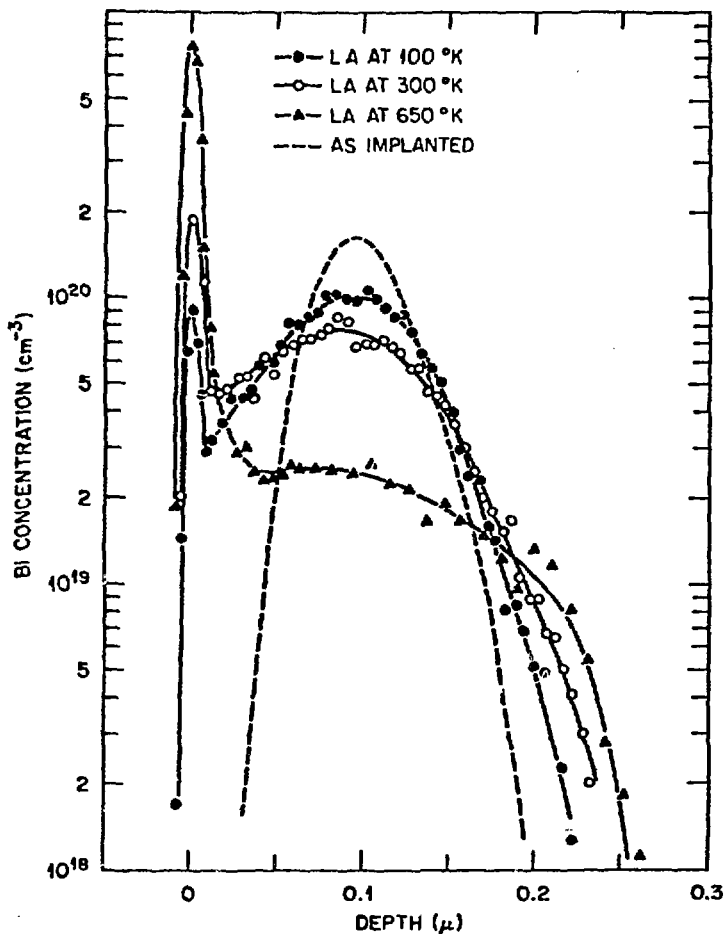


Figure 2. Profiles for ^{209}Bi (250 keV, $1.1 \times 10^{15}/\text{cm}^2$) in (100) Si After Annealing at Different Substrate Temperatures.

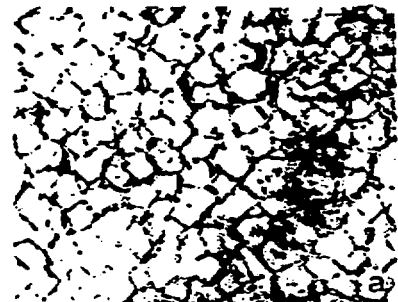
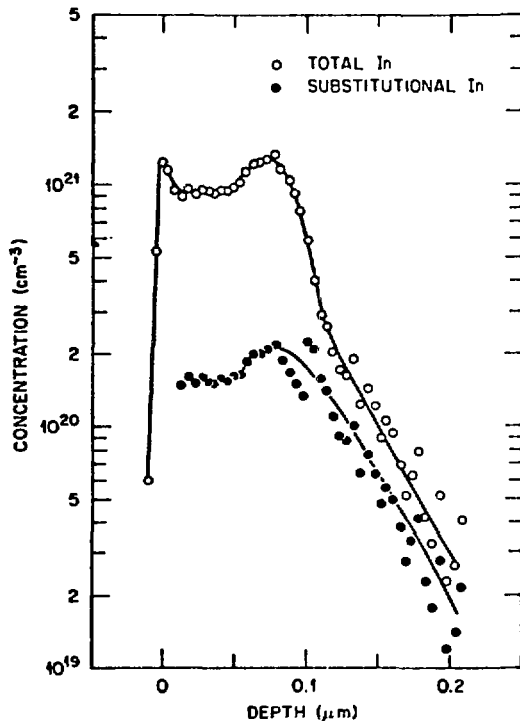
where we plot the total dopant concentration and the substitutional concentration as functions of depth after laser annealing. In Fig. 3, up to a concentration of $\sim 1.5 \times 10^{20}/\text{cm}^3$ the dopant is highly substitutional in the lattice, but in the near surface region where the total dopant concentration rises significantly above this, the substitutional concentration remains relatively constant. Therefore, the value of $1.5 \times 10^{20}/\text{cm}^3$ is the maximum substitutional solubility (C_S^{max}) for In in Si under these laser annealing conditions ($1.5 \text{ J}/\text{cm}^2$, $15 \times 10^{-9} \text{ sec}$. pulse duration time, growth velocity $\sim 4.5 \text{ m}/\text{sec}$).

Table I compares measured values for C_S^{max} for five different dopants in Si with the corresponding equilibrium solubility limits (C_S^0).⁹ Values for C_S^{max} exceed C_S^0 by factors that range from 4 in the case of As to over 500 in the case of Bi. These

results demonstrate the high degree of supersaturation that can be achieved in these alloy systems. Each system exhibits retrograde solubility in that on the equilibrium phase diagram the dopant has its maximum concentration at a temperature which is not a eutectic temperature. As shown by others,¹⁷ the retrograde maximum concentration cannot be exceeded during solidification unless there is deviation from conditions of local equilibrium at the interface. The large values for C_S^{\max} relative to C_S^0 therefore conclusively demonstrate the nonequilibrium nature of the laser annealing induced liquid phase epitaxial regrowth process. Dopant incorporation into the lattice during regrowth at these high velocities is by means of "solute trapping" as discussed by others.^{17,18}

Mechanisms Limiting Substitutional Solubility

Substitutional solubilities, achieved by pulsed laser annealing of ion implanted silicon, are limited by three mechanisms. The first of these is lattice strain, which dominates for the case of B in Si.¹⁹ When B goes substitutional in the silicon lattice during laser annealing, the lattice undergoes a one dimensional contraction in a direction normal to the surface.²⁰ Contraction causes strain in the lattice and the magnitude is proportional to the local B concentration. When the strain exceeds the fracture strength of Si (at a B concentration of ~4 atomic %)



0.2 μm

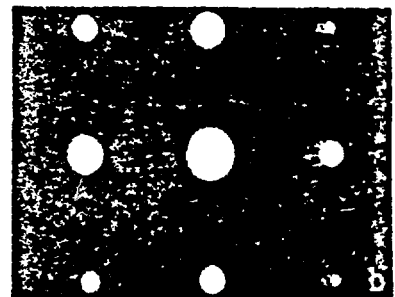


Figure 3. Profiles (left) and Microstructure (right) for ^{115}In (125 keV, $1.3 \times 10^{16}/\text{cm}^2$) in (100) Si After Laser Annealing.

cracks will develop in the implanted region.¹⁹ This is shown by the SEM photographs in Fig. 4. After annealing, cracks ($\sim 1 \mu$ wide) are observed in the implanted region. The cracks run the entire length of the sample (~ 1 cm) and penetrate to a depth of $\sim 1 \mu$. To reduce lattice strain and to increase the incorporated B concentration, it would be necessary to simultaneously incorporate a dopant which is known to give rise to a lattice expansion, possibly Ga.

The second mechanism limiting substitutional solubility during laser annealing is the interfacial instability during regrowth which leads to lateral segregation of rejected dopant and the formation of a well defined cell structure in the near surface region after annealing.¹¹ This mechanism dominates for the case of Ga and In and probably Bi. An example of the cell structure is shown in the TEM micrograph of Fig. 3 for In implanted Si. After laser annealing the TEM micrograph shows the presence of a well defined cell structure in the near surface region. The interior of each cell is a defect-free epitaxial column of silicon extending to the surface. Trapped substitutionally within the lattice of these columns is the substitutional In in the near surface region. Surrounding each column of silicon is a thin cell wall ($\sim 50 \text{ \AA}$ wide) containing large concentrations of segregated In. The cell walls penetrate to a depth of $\sim 1000 \text{ \AA}$ and contain the nonsubstitutional In in the near surface region. Diffraction patterns from this crystal contain weak extra spots which arise from crystalline In in the cell walls. This demonstrates nucleation of the second phase during laser annealing.

The interfacial instability which leads to the formation of a well defined cell structure is due to constitutional supercooling at the liquid-solid interface during regrowth.¹¹ This is a well recognized and long studied phenomena in normal crystal growth from the liquid.²¹ In laser annealing effects due to constitutional supercooling are observed on a much finer scale due to the high velocity of the liquid-solid interface.

Constitutional supercooling arises due to the pile up of segregated dopant at the interface.²¹ The concentration gradient of rejected dopant in the liquid leads to a gradient of the freezing temperature of the liquid in front of the interface. If the actual temperature gradient in the liquid is less than the gradient of the freezing temperature, then a region in front of the interface will be supercooled since the actual temperature is less than the liquidus temperature. Under these conditions, a perturbation on a planar interface can become unstable and grow, leading to lateral segregation of dopant and the formation of a cell structure. To delay the onset of

interfacial instability and increase the maximum substitutional solubility, it would be necessary to increase the thermal gradient in the liquid. This would require higher growth velocities.

The third mechanism limiting substitutional solubility is the fundamental thermodynamic limit for solute trapping. Predictions of this limit have been made by Cahn et al.¹⁴ On a plot of the Gibbs Free Energy α a function of composition (at fixed temperature) the solid and liquid lines intersect at one point which provides an upper limit for the solid composition which can form from the liquid at any composition. Plotting the locus of these points at different temperatures on the equilibrium phase diagram (schematically illustrated in Fig. 5) determines the T_0 curve,¹⁴ which is the maximum solidus composition which can be formed from the liquid, even at infinite growth velocity. For retrograde systems,



Figure 4. Cracks in the Surface Region of ^{11}B (35 keV, $6 \times 10^{16}/\text{cm}^2$) Implanted (100) Si After Laser Annealing.

Table II. Comparison of Maximum Substitutional Dopant Concentrations After Laser Annealing at Two Substrate Temperatures (300 K and 77 K) to Predicted Thermodynamic Limits to Solute Incorporation (C_S^L).

Dopant	C_{300}^{\max} (cm^{-3})	C_{77}^{\max} (cm^{-3})	C_S^L (cm^{-3})
As	6.0×10^{21}	6.0×10^{21}	5×10^{21}
Sb	1.3×10^{21}	---	3×10^{21}
Ga	4.5×10^{20}	8.8×10^{20}	6×10^{21}
In	1.5×10^{20}	2.8×10^{20}	2×10^{21}
Bi	4×10^{20}	1.1×10^{21}	1×10^{21}

a simple estimate can be made for the maximum composition on the T_0 curve, as shown in Ref. 14. This maximum composition, (C_S^0) is given by the liquidus composition at a temperature corresponding to the retrograde temperature on the equilibrium phase diagram (see Fig. 5).

Predictions of the limiting composition (C_S^0) are given in Ref. 14 and listed in Table II for the five dopants we have studied. Listed also in Table II are measured values for maximum substitutional solubilities obtained using laser annealing conditions designed to result in two different growth velocities. Annealing at 300 K gives rise to a growth velocity of ~ 4.5 m/sec, whereas annealing at 77 K results in a growth velocity of ~ 6.0 m/sec. At either growth velocity, the maximum substitutional concentrations are approaching thermodynamic limits. In the case of Ga, In, and Bi, the substitutional concentrations can be increased by factors of 2-3 at a growth velocity of 6 m/sec (77 K) compared to results achieved at 4.5 m/sec (300 K). These concentrations are limited by interfacial instability and these results show that the onset of instability can be delayed somewhat by going to higher velocities as expected. At the higher growth velocity the concentration of Bi in substitutional lattice sites exceeds the equilibrium solubility limit by over three orders of magnitude. Finally, for As in Si there is no increase in the measured maximum substitutional concentrations as the growth velocity is increased. This indicates that the thermodynamic limit for As in Si may have been reached. The fact that the measured limit exceeds the predicted limit is probably due to uncertainties on the equilibrium phase diagram from which the predictions were made.

Conclusions

In pulsed laser annealing of ion implanted silicon, Group III and V dopants are trapped into substitutional lattice sites at concentrations that can be far greater than equilibrium solubility limits. Values for k' and C_S^{\max} far exceed corresponding equilibrium values. Both k' and C_S^{\max} are found to be functions of growth velocity. For most dopants, substitutional solubility is limited by interfacial instability during regrowth or by lattice strain. For As in Si, the thermodynamic limit to dopant incorporation may have been reached.

References

1. See for example, C. W. White, J. Narayan and R. T. Young, Science 204, 461 (1979) and references contained therein.

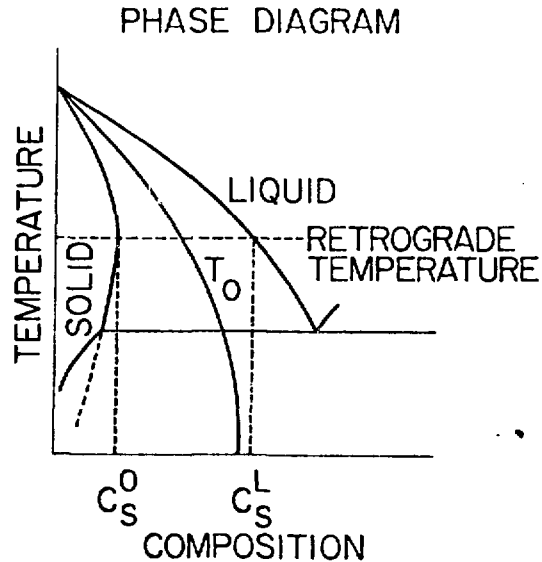


Figure 5. Phase Diagram (schematic) Showing T_0 Curve, C_S^0 and C_S^L .

2. Laser-Solid Interactions and Laser Processing-1978, (ed. by S. D. Ferris, H. J. Leamy and J. M. Poate, AIP Conference Proceedings No. 50, American Institute of Physics, New York, 1979).
3. Laser and Electron Beam Processing of Materials, (ed. by C. W. White and P. S. Peercy, Academic Press, New York, 1980).
4. J. Narayan, R. T. Young and C. W. White, *J. Appl. Phys.* **49**, 3912 (1978).
5. J. C. Bean, H. J. Leamy, J. M. Poate, G. A. Rozgonyi, T. T. Sheng, J. S. Williams and G. K. Celler, *Appl. Phys. Lett.* **33**, 227 (1978).
6. R. T. Young and J. Narayan, *Appl. Phys. Lett.* **33**, 14 (1978).
7. J. Narayan, R. T. Young, R. F. Wood and W. H. Christie, *Appl. Phys. Lett.* **33**, 338 (1979).
8. B. R. Appleton, B. C. Larson, C. W. White, J. Narayan, S. R. Wilson and P. P. Pronko, Ref. 2, p. 291.
9. C. W. White, S. R. Wilson, B. R. Appleton and F. W. Young, Jr., *J. Appl. Phys.* **51**, 738 (1980).
10. C. W. White, S. R. Wilson, B. R. Appleton, F. W. Young, Jr. and J. Narayan, Ref. 3, p. 111.
11. C. W. White, S. R. Wilson, B. R. Appleton and J. Narayan, Ref. 3, p. 124.
12. D. H. Auston, J. A. Golovchenko, A. L. Simons, R. E. Slusher, P. R. Smith, C. M. Surko and T.N.C. Venkatesan, Ref. 2, p. 11.
13. R. F. Wood, J. C. Wang, G. E. Giles and J. R. Kirkpatrick, Ref. 3, p. 37.

14. J. W. Cahn, S. R. Coriell and W. J. Boettinger, Ref. 3, p. 89.
15. C. W. White, P. P. Pronko, S. R. Wilson, B. R. Appleton, J. Narayan and R. T. Young, J. Appl. Phys. 50, 3261 (1980).
16. F. Trumbore, Bell System Tech. Journal 39, 205 (1960).
17. J. C. Baker and J. W. Cahn, Acta. Metall. 17, 575 (1969).
18. K. A. Jackson, G. H. Gilmer and H. J. Leamy, Ref. 3, p. 104.
19. C. W. White, J. Narayan and R. T. Young, Ref. 2, p. 275.
20. B. C. Larson, C. W. White and B. R. Appleton, Appl. Phys. Lett. 32, 801 (1978).
21. See for example, K. A. Jackson in Treatise on Solid State Chemistry, Vol. 5, (ed. by N. B. Hannay, Plenum Press, New York, 1975), Chapter 5.